Isothermal and Thermomechanical Fatigue Behaviour of IN738LC

S. Yandt[1*], D.Y. Seo[1], P. Au[1], J. Beddoes[2]
[1]*National Research Council Canada – IAR, Ottawa Ontario, Canada;* [2]*Carleton University, Ottawa, Canada*

Abstract

The isothermal low-cycle fatigue (IT-LCF) and the in-phase (IP) and out-of-phase (OP) thermomechanical fatigue (TMF) life of IN738LC nickel-base superalloy was investigated in the temperature range of 750ºC to 950ºC. The experimental results indicate that fatigue life depends on strain-temperature phasing and mechanical strain range. In-phase TMF tests exhibited lives that were similar to the strain-life data obtained from IT-LCF tests conducted at 950°C. A crossover of IP and OP-TMF strain-life curves, where OP-TMF resulted in the longest life at high-strain ranges and shortest life at low-strain ranges, was also observed. Under all test conditions fatigue cracks nucleated at surface connected grain boundaries and propagated along grain boundaries. Extensive creep cavitation and intergranular damage were observed in IP-TMF test specimens. A higher density of surface-connected fatigue cracks was observed for IT-LCF and IP-TMF loading conditions than for OP-TMF.

1 Introduction

The first stage nozzle guide vanes and blades in a gas turbine are subjected to thermomechanical fatigue (TMF) conditions that involve complex thermal and mechanical loading cycles, in which interactions occur between fatigue and other high temperature damage mechanisms, such as creep and oxidation. These interactions cannot be adequately predicted nor identified from isothermal low-cycle fatigue (LCF) material behaviour [1,2]. Understanding such interactions is crucial for developing material constitutive models and component life prediction tools for the design and lifecycle management of these critical parts. Clearly, experimental data which more closely emulates the temperature and mechanical loading history for these components is required and thermomechanical fatigue testing techniques have been developed for this purpose.

In laboratory TMF tests, the temperature and mechanical loading can be programmed and controlled independently to simulate complex thermal and mechanical loading histories. However, in general, in-phase (IP) and out-of-phase (OP) TMF loading histories are used in laboratory studies and isothermal low-cycle fatigue (IT-LCF) tests may also be conducted at the maximum and minimum temperatures corresponding to the TMF tests to establish baselines. In

* Email: scott.yandt@nrc-cnrc.gc.ca

the above approach, a number of researchers have observed a crossover of the IP and OP-TMF strain-life curves for nickel-base superalloys [3-5]. This crossover is characterized by IP-TMF life being shorter than OP-TMF at high strain ranges, while IP-TMF life is longer than OP-TMF at low strain ranges. However, this crossover does not appear to be a universal behaviour for nickel-base superalloys since Chen and coworkers [6] have reported that OP-TMF lives were shorter than IP-TMF lives for IN738LC. It has been speculated that the crossover of the strain-life curves is a result of the relative contributions of fatigue, creep and oxidation damage mechanisms to the overall fatigue life [4].

Isothermal-LCF tests are used as a baseline for TMF tests since it is anticipated that these tests, when conducted at the maximum test temperature, represent the most detrimental loading conditions, and therefore will result in conservative estimates for fatigue life under transient thermal and mechanical loading conditions. On the contrary, numerous investigators [1,7-9] have reported that IT-LCF tests do not result in conservative life predictions for IP and OP-TMF tests at the same mechanical strain levels. Other investigators [6,10,11] have found that IT-LCF tests provide an adequate estimate for either IP or OP-TMF life, but not for both.

This paper considers the fatigue behaviour of the nickel-base superalloy IN738LC under isothermal and OP and IP-TMF loading conditions. Thermomechanical fatigue experiments were conducted in the temperature range of 750°C to 950°C and IT-LCF tests were performed at 950°C. The cyclic deformation response and fatigue life for IT-LCF and TMF test conditions is reported. A detailed microstructural analysis of the fatigue samples was undertaken to identify the crack nucleation and propagation modes, microstructural changes and the dominant damage mechanisms.

2 Experimental Procedures

The nominal chemical composition for IN738LC is presented in Table 1. The material was obtained from a commercial foundry in the form of 200×125×19 mm investment cast plates that were hot isostatically pressed for 4 hours at 1205°C and 103.4 MPa to reduce interdendritic casting porosity. The material was heat treated using the standard solution and aging heat treatment specified for IN738LC: 1120°C for 2 hours AC + 845°C for 24 hours AC. Application of this heat treatment resulted in a bimodal γ' precipitate distribution consisting of approximately 0.5 μm primary and 80 nm secondary γ', with approximately 40% volume fraction as shown in Figure 1a. Discrete MC carbides with a script morphology were also observed in interdendritic regions and along grain boundaries as shown in Figure 1b.

For fatigue testing, smooth cylindrical specimens with a gage length of 33.0 mm and a gage section diameter of 7.62 mm were machined from the heat-treated

material. Details of the specimen dimensions are shown in Figure 2. The same specimen geometry was used for both IT-LCF and TMF experiments.

Table 1 – Nominal chemical composition for IN738LC in Wt%.

Ni	Cr	Co	Al	Ti	W	B	Ta	Mo	Zr	Nb	C
Bal.	16	8.5	3.5	3.5	2.6	0.01	1.8	1.8	0.04	0.9	0.1

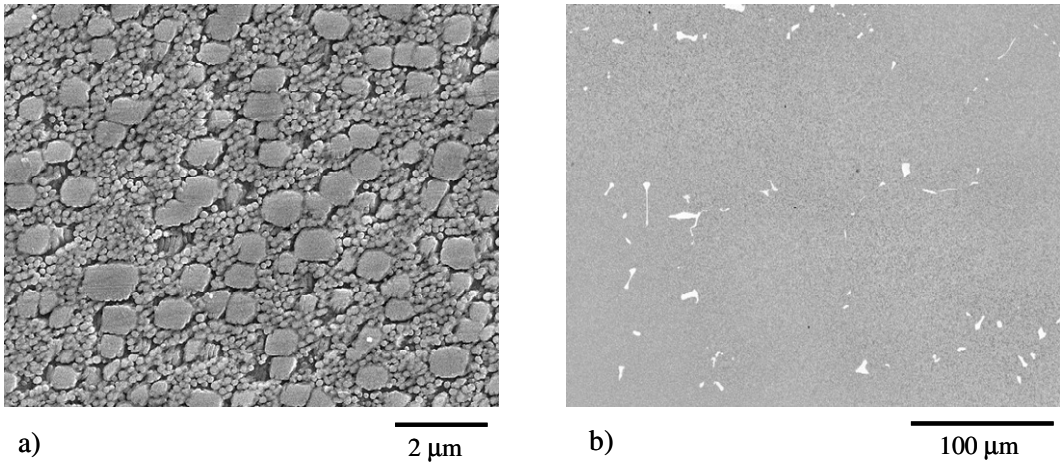

Figure 1 – Microstructure of IN738LC after application of standard heat treatment; a) SEM secondary electron image showing bimodal γ' precipitates and b) SEM back-scatter image showing grain boundary and interdendritic MC carbides.

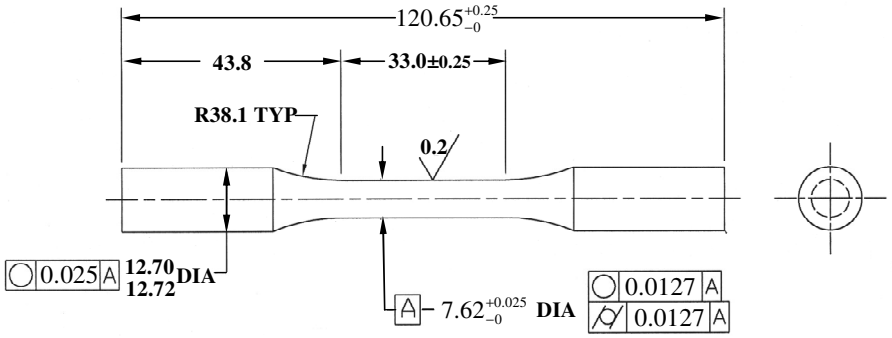

Figure 2 – Schematic drawing of specimen geometry. The specimen dimensions are in mm.

Fatigue experiments were conducted in an MTS 810 servo-hydraulic test machine under closed-loop strain control using triangular waveforms for mechanical strain and temperature control functions. Specimens were heated using high frequency induction heating. The induction heating coil design was optimized so as to ensure that the axial and circumferential temperature gradients were reduced to ±10°C within the controlled gage section under static conditions for IT-LCF tests and under dynamic conditions during TMF tests. Forced cooling was not used during the TMF experiments. A two-colour infrared pyrometer was used for closed-loop temperature control. During TMF tests the total strain, that is the sum of the mechanical (ε_m) and thermal strain (ε_{th}), was used as the control function. The thermal strain function was obtained prior to commencing a TMF test by recording the thermal strain response during several thermal cycles performed

under zero load-control. During analysis of the test data the mechanical strain was obtained by subtracting the recorded thermal strain function from the total strain. An axial high-temperature extensometer with a gage length of 12 mm was used for closed-loop control of the total strain. A computer controlled data acquisition system was used to generate the temperature and total strain command waveforms and to acquire data during the experiments. Additional details on the experimental setup and testing procedures are described elsewhere [12].

The TMF experiments were performed with a temperature range of 750°C to 950°C. The IT-LCF tests were performed at 950°C. The TMF and isothermal experiments were conducted using fully reversed (R_ε = -1) mechanical strain ranges of 1.0, 0.8, 0.6 and 0.45%. A constant mechanical strain rate (2×10^{-5} sec^{-1}) was used during the TMF and IT-LCF tests. For the TMF experiments, in-phase and out-of-phase cycles in which the maximum mechanical strain coincided with the maximum and minimum temperature, respectively, were used. The fatigue experiments were concluded after a 5% tensile load drop from the stabilized tensile load amplitude was observed.

Microstructural characterization was performed on the material from the tested fatigue specimens as well as from the cast plate. Metallographic samples were prepared using standard metallographic techniques. Selected samples were etched electrolytically in a solution of 12 ml H_3PO_4 + 40 ml HNO_3 + 48 ml H_2SO_4 to reveal the γ' precipitate morphology. A Philips XL30S-FEG scanning electron microscope (SEM) was employed to study the fracture surfaces and longitudinal metallographic sections of test specimens to identify crack nucleation sites, crack propagation paths and microstructural changes.

3 Results

3.1 Cyclic Material Behaviour

The cyclic stress-mechanical strain hysteresis loops representative of OP and IP-TMF and IT-LCF tests conducted at 1% mechanical strain range are shown in Figure 3. It may be noted that hysteresis loops for the first cycle and at half-life are included to illustrate the evolution of the cyclic stress-mechanical strain response. The IP and OP-TMF hysteresis loops are asymmetric; however, they are similar in shape and appear to be in rotated 180° about the origin with respect to each other. The stress range for IP and OP-TMF tests were observed to be similar. Out-of-phase TMF cycling resulted in a tensile mean stress, whereas IP-TMF tests exhibited a compressive mean stress. The hysteresis loops for IT-LCF tests were observed to be symmetrical about the abscissa and had negligible mean stress. A comparison of the hysteresis loops between the first cycle and half-life for each loading case shows that IT-LCF tests exhibited cyclic softening, while the stress range remained predominantly constant during TMF loading.

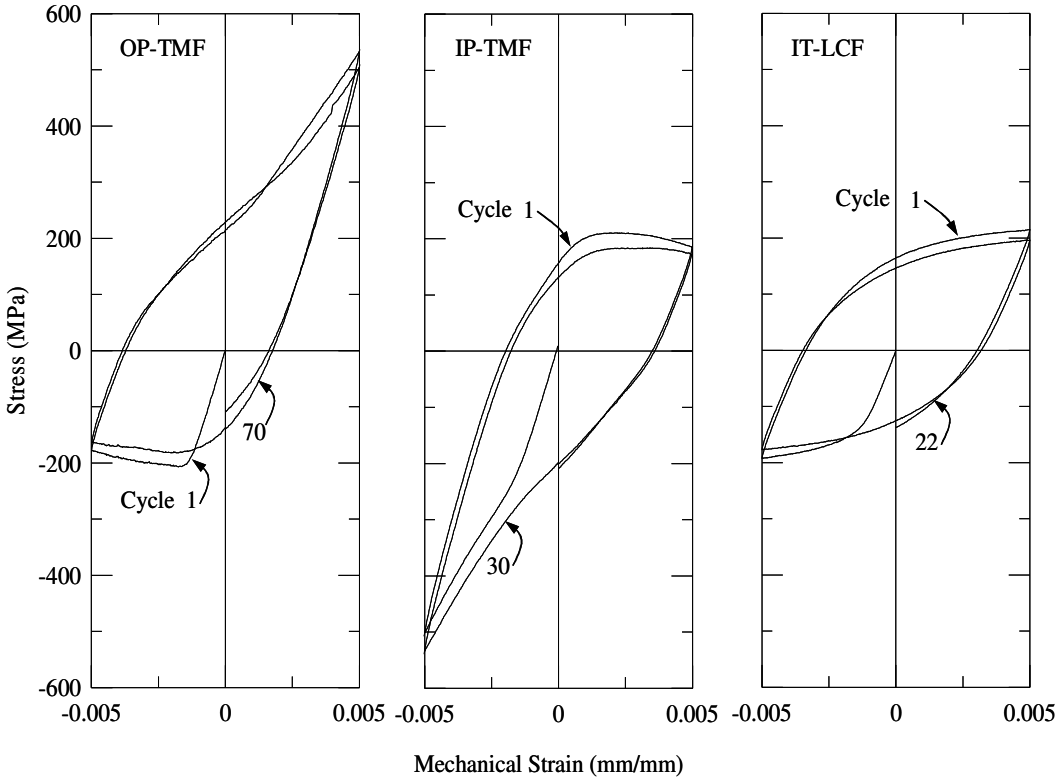

Figure 3 – First cycle and half-life stress-mechanical strain hysteresis loops for OP-TMF, IP-TMF and IT-LCF tests, $\Delta\varepsilon_m$ = 1.0%.

3.2 Cyclic Life

Experimental results for IT-LCF, OP-TMF and IP-TMF tests are presented as mechanical strain-life curves in Figure 4. The results indicate that OP-TMF loading produces longer lives than IP-TMF and IT-LCF loading (as high as 2 times) at high mechanical strain ranges ($\Delta\varepsilon_m$ = 1.0%). In-phase TMF and IT-LCF loading results in longer fatigue lives than OP-TMF (as high as 2 times) at low mechanical strain ranges ($\Delta\varepsilon_m$ = 0.45%). At intermediate mechanical strain ranges ($\Delta\varepsilon_m \approx 0.65\%$) a crossover of the OP-TMF and IP-TMF mechanical-strain life curves was observed. It is interesting to note that the IP-TMF tests exhibited longer fatigue lives than the IT-LCF tests for all mechanical strain ranges tested in this investigation.

The inelastic strain range ($\Delta\varepsilon_{in}$) versus life for the IT-LCF, IP-TMF and OP-TMF tests is shown in Figure 5. The results show that on the basis of inelastic strain the IT-LCF tests exhibited longer lives than the IP-TMF tests and the crossover of the IP-TMF and OP-TMF inelastic strain-life curves is more evident. The OP-TMF tests exhibited longer lives (as high as 2.3 times) at high inelastic strain ranges and shorter lives (as high as 3 times) at low inelastic strain ranges when compared with the IP-TMF tests.

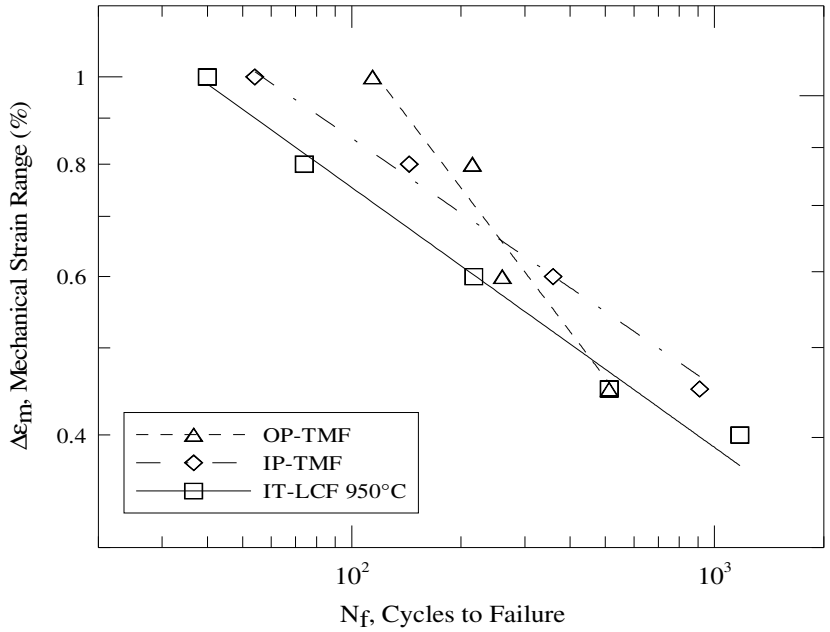

Figure 4 – Mechanical strain range versus life for OP-TMF, IP-TMF and IT-LCF tests.

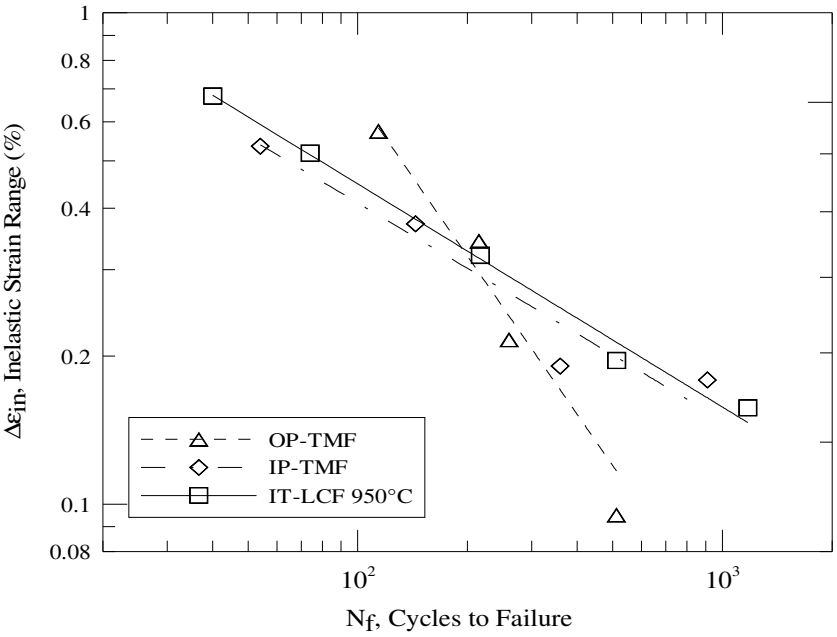

Figure 5 – Inelastic strain range versus life for OP-TMF, IP-TMF and IT-LCF tests.

To differentiate between loading conditions (TMF versus IT-LCF) and the resulting inelastic strain response, the inelastic strain range was plotted versus mechanical strain range for the IT-LCF, OP-TMF and IP-TMF tests, as shown in Figure 6. The results show that the inelastic strain ranges for the IP and OP-TMF tests conditions were similar and in both cases they were significantly lower than that developed during the IT-LCF tests.

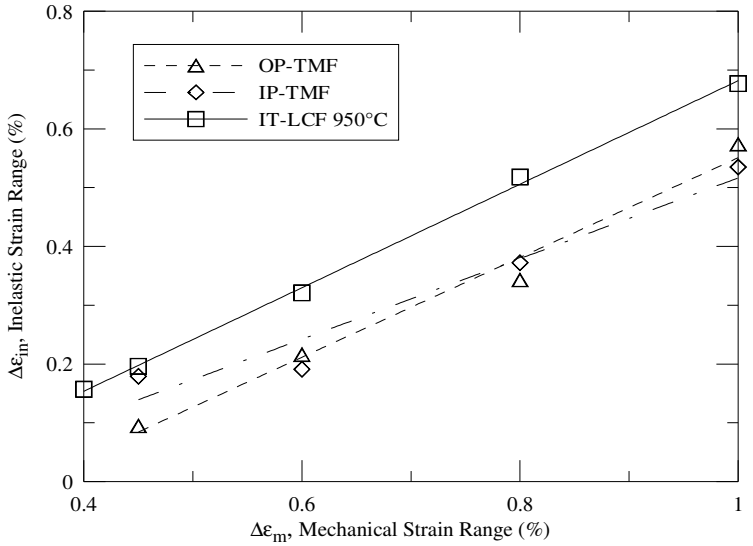

Figure 6 – Inelastic strain range versus mechanical strain range for OP-TMF, IP-TMF and IT-LCF tests.

3.3 Metallographic Examination

Post-test examination of fatigue samples showed surface oxides accompanied by a γ' depleted zone, and preferential oxidation of surface-connected grain boundaries. Representative micrographs exhibiting these features are shown in Figure 7. These microstructural features were also observed in surface-connected fatigue cracks. Crack nucleation sites for all isothermal and TMF tests were predominantly intergranular and were observed to coincide with the oxidized surface connected grain boundaries. Crack propagation was predominantly intergranular in most specimens.

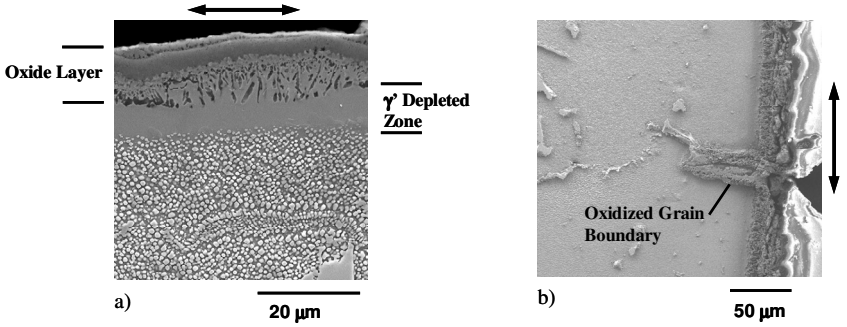

Figure 7 – SEM micrographs showing environmental damage; a) surface oxide layer, internal oxidation and γ' depleted zone (IT-LCF 950°C, $\Delta\varepsilon_m$ = 0.45%) and b) oxidized surface-connected grain boundary (OP-TMF 750-950°C, $\Delta\varepsilon_m$ = 0.45%). Arrows indicate the loading direction.

In-phase TMF test specimens exhibited extensive creep cavitation and sub-surface internal intergranular cracking, as shown in Figure 8, which was not observed in specimens tested under IT-LCF and OP-TMF conditions. In addition to the forgoing microstructural features, a qualitative optical examination of the specimen surface showed a substantially higher density of surface connected

cracks in the IT-LCF and IP-TMF test samples than those tested under OP-TMF cycling.

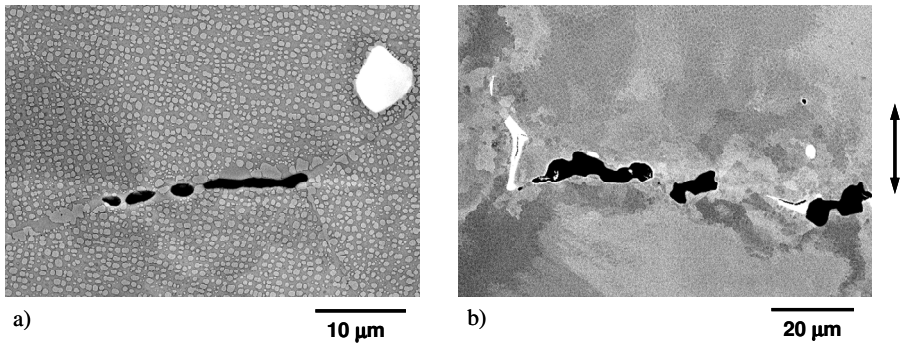

Figure 8 – SEM micrographs showing intergranular cavitation observed after IP-TMF; a) 750-950°C $\Delta\varepsilon_m$ = 1.0% and b) 750-950°C $\Delta\varepsilon_m$ = 0.45%. Arrow indicates loading direction.

4 Discussion

The mechanical strain-life and inelastic strain-life curves shown in Figures 4 and 5, respectively, show a crossover in the IP and OP-TMF life curves. Similar findings have been reported for other nickel-base superalloys [3-5], although results from a study undertaken by Chen and coworkers [6] using IN738LC and tests conditions almost identical to those employed in this study, did not exhibit a crossover in the TMF strain-life curves. The crossover in the strain-life curves can be rationalized by considering the relative contributions of different damage mechanisms.

In the absence of high temperature damage mechanisms, such as creep and oxidation, the LCF and TMF life can be characterized on the basis of the inelastic strain range, i.e. based solely on fatigue damage. Figure 6 compares the inelastic strain range versus the mechanical strain range for the isothermal and TMF test conditions. The following observations can be made. First, the IP and OP-TMF tests both exhibit similar inelastic strain ranges, and therefore both tests conditions should have similar fatigue lives when fatigue damage is considered. However, the strain-life results for IP and OP-TMF presented in Figures 4 and 5 show otherwise. Second, the inelastic strain range was smaller for TMF loading than IT-LCF, when compared at the same mechanical strain range, and therefore the TMF tests should exhibit longer lives than IT-LCF based on fatigue damage. When experimental scatter is taken into consideration, IP-TMF and IT-LCF exhibit similar fatigue lives, again contradicting what one would intuitively conclude from the results presented in Figure 6. The fact that IT-LCF and TMF lives coincide is probably coincidental since the constitutive material response and deformation mechanisms are different between TMF and IT-LCF loading conditions.

Microstructural analysis of the IT-LCF and IP and OP-TMF test samples show that fatigue crack nucleation and propagation mechanisms were similar under each loading condition. Oxidation and γ' depleted zones were observed on the

fracture surfaces and ahead of propagating fatigue cracks, indicating that crack nucleation and propagation were environmentally assisted. Since TMF tests were intermittently exposed to the maximum test temperature, when compared to IT-LCF tests, it is expected that environmentally induced oxidation damage will be more severe for IT-LCF than for TMF tests of the same duration. Examination of fatigue samples showed that the density of surface connected crack nucleation sites was larger for IT-LCF and IP-TMF than OP-TMF. One may infer that the crack nucleation phase consumes a small fraction of the OP-TMF life, and therefore the majority of fatigue life is spent in propagating the fatigue crack to failure. Creep cavitation and intergranular cracking was observed solely in IP-TMF tests specimens (see Figure 8), suggesting that creep was the dominant damage mechanism for this particular loading condition.

At high strain ranges, the longer life exhibited by OP-TMF tests, when compared with IT-LCF tests, is probably due to a larger portion of cyclic life spent in nucleating fatigue cracks than in IT-LCF tests. In OP-TMF tests tensile loading occurs during the low temperature portion of the thermal cycle (at 750°C) where the fatigue crack propagation rate has been reported to be higher than at 850ºC in IN738LC [13]. One may infer that the shorter life exhibited by OP-TMF tests at low strain ranges, when compared to IP-TMF and IT-LCF tests, is the result of higher fatigue crack propagation rates. At high strain ranges, the lower cyclic life of IP-TMF tests, when compared to OP-TMF tests, is probably due to the contribution of creep damage during IP-TMF loading. It is speculated that the contribution of creep damage is reduced at low strain ranges under IP-TMF, and therefore IP-TMF tests exhibit longer lives than OP-TMF at low strain ranges.

5 Conclusions

In this paper the fatigue behaviour of the nickel-base superalloy IN738LC was investigated using IP and OP-TMF cycles and under IT-LCF loading conditions. The fatigue lives for OP-TMF were longer at high mechanical strain ranges than IT-LCF and IP-TMF; this trend was reversed at low mechanical strain ranges. Detailed microstructural analysis of tested fatigue specimens was undertaken to identify the mechanisms for fatigue crack nucleation and propagation and the dominant damage mechanisms. Crack nucleation occurred at preferentially oxidized surface-connected grain boundaries and then propagated along grain boundaries oriented normal to the mechanical loading direction. The fatigue lives under TMF and IT-LCF loading conditions can not be rationalized solely based on fatigue damage accumulation. Oxidation products and γ' depletion were observed both on the surface of the fatigue specimens and along the surface of fatigue cracks indicating that fatigue was environmentally assisted. Creep cavitation and sub-surface intergranular cracking was observed in IP-TMF test specimens, suggesting that creep was the dominant damage mechanism for this particular loading condition. The interactions of the above mechanisms must be taken into account when developing constitutive material models and life prediction algorithms.

6 References

[1] J.-Y. Guedou, Y. Honnorat, Thermomechanical Fatigue of Turbo-Engine Blade Superalloys, in: H. Sehitoglu (Ed.), Thermomechanical Fatigue Behavior of Materials ASTM STP 1186, American Society for Testing and Materials, Philadelphia PA, 1993, pp. 157-175

[2] E. Fleury, L. Remy, Behavior of Nickel-Base Superalloy Single Crystals under Thermal-Mechanical Fatigue, Met. Trans A 25A (1994) 99-109

[3] R.C. Bill, M.J. Verrilli, M.A. McGaw, G.R. Halford, Preliminary Study of Thermomechanical Fatigue of Polycrystalline Mar-M200, AVSCOM Technical Report 83-C-6, 1984

[4] D.A. Boismier, H. Sehitoglu, Thermo-Mechanical Fatigue of Mar-M247: Part 1 – Experiments, J. Eng. Mat. Tech., Trans. ASME 112 (1990) 68-79

[5] Y. Kadioglu, H. Sehitoglu, Thermomechanical and Isothermal Fatigue Behavior of Bare and Coated Superalloys, J. Eng. Mat. Tech., Trans. ASME 117 (1995) 94-102

[6] H. Chen, W. Chen, D. Mukherji, R.P. Wahi, H. Wever, Cyclic Life of Superalloy IN738LC Under In-Phase and Out-of-Phase Thermo-mechanical Fatigue Loading, Z. Metallkd 86(6) (1999) 423-427

[7] T. Beck, G. Pitz, K.-H. Lang, D. Lohe, Thermal-Mechanical and Isothermal Fatigue of IN 792 CC, Mat. Sci. Eng. A 234 (1997) 719-722

[8] P. Pototzky, H.J. Maier, H.-J. Christ, Thermomechanical Fatigue Behavior of the High-Temperature Titanium Alloy IMI 834, Met. Trans. A 29A (1998) 2995-3004

[9] K.D. Sheffler, Vacuum Thermal-Mechanical Fatigue Behavior of Two Iron-Base Alloys, in: D.A. Spera, D.F. Mowbray (Eds.), Thermal Fatigue of Materials and Components ASTM STP 612, American Society for Testing and Materials, Philadelphia PA, 1976, pp. 214-226

[10] J. Komenda, L. Linde, P.J. Henderson, Microstructural Aspects of Damage Occurring During Thermo-mechanical and Low Cycle Fatigue Testing of an Oxide Dispersion Strengthened Alloy, in: J. Bressers, L. Remy (Eds.), Fatigue Under Thermal and Mechanical Loading, Kluwer Academic Publishers, Netherlands, 1996, pp. 339-347

[11] B. Kleinpass, K.-H., Lang, D. Lohe, E. Macherauch, Thermal-Mechanical Fatigue Behavior of NiCr22Co12Mo9, in: J. Bressers, L. Remy (Eds.), Fatigue Under Thermal and Mechanical Loading, Kluwer Academic Publishers, Netherlands, 1996, pp. 327-337

[12] S. Yandt, Development of a Thermal-Mechanical Fatigue Testing Facility, Masters thesis, Carleton University, Ottawa, 2000

[13] R.B. Scarlin, Fatigue Crack Growth in a Cast Ni-Base Alloy, Mat. Sci. Eng. 21 (1975) 139-147